

CogBlender: Towards Continuous Cognitive Intervention in Text-to-Image Generation

SHENGQI DANG, Tongji University and Shanghai Innovation Institute, China

JIAYING LEI, Tongji University, China

YI HE, Tongji University, China

ZIQING QIAN, Tongji University, China

NAN CAO*, Tongji University and Shanghai Innovation Institute, China



Input prompt: A girl is reading a book in the room.

Fig. 1. CogBlender is a framework designed to intervene in the continuous cognitive properties during the text-to-image generation process.

Beyond conveying semantic information, an image can also manifest cognitive attributes that elicit specific cognitive processes from the viewer, such as memory encoding or emotional response. While modern text-to-image models excel at generating semantically coherent content, they remain limited in their ability to control such cognitive properties of images (e.g., valence, memorability), often failing to align with the specific psychological intent. To bridge this gap, we introduce CogBlender, a framework that enables continuous and multi-dimensional intervention of cognitive properties during text-to-image generation. Our approach is built upon a mapping between the *Cognitive Space*, representing the space of cognitive properties, and the *Semantic Manifold*, representing the manifold of the visual semantics. We define a set of *Cognitive Anchors*, serving as the boundary points for the cognitive space. Then we reformulate the velocity field within the

flow-matching process by interpolating from the velocity field of different anchors. Consequently, the generative process is driven by the velocity field and dynamically steered by multi-dimensional cognitive scores, enabling precise, fine-grained, and continuous intervention. We validate the effectiveness of CogBlender across four representative cognitive dimensions: valence, arousal, dominance, and image memorability. Extensive experiments demonstrate that our method achieves effective cognitive intervention. Our work provides an effective paradigm for cognition-driven creative design.

CCS Concepts: • **Computing methodologies** → Cognitive science; **Computer vision tasks**; **Image manipulation**.

Additional Key Words and Phrases: Text-to-image generation, emotion model, image memorability, cognitive property of image

ACM Reference Format:

Shengqi Dang, Jiaying Lei, Yi He, Ziqing Qian, and Nan Cao*. 2026. CogBlender: Towards Continuous Cognitive Intervention in Text-to-Image Generation. *ACM Trans. Graph.* 1, 1 (March 2026), 10 pages. <https://doi.org/10.1145/nnnnnnn.nnnnnnn>

1 Introduction

When an observer views an image, they engage in a multifaceted suite of responses, including affective appraisal, social inference, and intellectual curiosity [Cavanagh 2011; Gilbert and Li 2013]. These reactions are underpinned by fundamental cognitive processes, including perception, memory, and reasoning, which collectively synthesize the visual stimuli into a coherent mental representation [Kim et al. 2021; Neisser 2014; Szczepanowski et al. 2013]. In the domain of

* Nan Cao is the corresponding author.

Authors' Contact Information: Shengqi Dang, Tongji University and Shanghai Innovation Institute, Shanghai, China, dangsq123@163.com; Jiaying Lei, Tongji University, Shanghai, China, jiaying.lei@outlook.com; Yi He, Tongji University, Shanghai, China, heyi.hy11@gmail.com; Ziqing Qian, Tongji University, Shanghai, China, 2411920@tongji.edu.cn; Nan Cao*, Tongji University and Shanghai Innovation Institute, Shanghai, China, nan.cao@gmail.com.

Permission to make digital or hard copies of all or part of this work for personal or classroom use is granted without fee provided that copies are not made or distributed for profit or commercial advantage and that copies bear this notice and the full citation on the first page. Copyrights for components of this work owned by others than the author(s) must be honored. Abstracting with credit is permitted. To copy otherwise, or republish, to post on servers or to redistribute to lists, requires prior specific permission and/or a fee. Request permissions from permissions@acm.org.

© 2026 Copyright held by the owner/author(s). Publication rights licensed to ACM.

ACM 1557-7368/2026/3-ART

<https://doi.org/10.1145/nnnnnnn.nnnnnnn>

human-centered design, this foundation is pivotal: design objectives are increasingly defined by their capacity to modulate high-level human cognition. For example, expert designers carefully design images not just to be clear, but to trigger specific cognitive reactions, such as enhancing image memorability in artworks or fostering affective empathy in advertising [Davis and Bainbridge 2023; Septianto et al. 2021].

Although recent studies have begun to investigate "cognitive image properties" or "cognitive properties of images" [Chen et al. 2025; Goetschalckx et al. 2019], to the best of our knowledge, a formal and authoritative definition of this concept is still emerging. We define the cognitive properties of images as high-level evaluative attributes that arise from the interaction between visual stimuli and human cognitive processes, characterized by a measurable degree of inter-subject consistency. Crucially, these properties are (1) multi-dimensional, inhabiting a latent psychological space of interacting facets (e.g., multi-dimensional emotion model [Bradley and Lang 1994]); and (2) continuous, manifesting as a spectrum of intensities rather than discrete categories.

While modern text-to-image (T2I) models excel in semantic fidelity, aligning generation with high-order cognitive properties remains an open challenge. Pioneering works like GANalyze [Goetschalckx et al. 2019] navigated single-dimensional intervention on the latent space of Generative adversarial network (GAN), and recent frameworks such as EmotiCrafter [Dang et al. 2025] enabled continuous two-dimensional emotion modulation. However, three critical bottlenecks persist: (1) The relationship between abstract cognitive properties and visual features is inherently non-linear and significantly more entangled than standard object-level alignment. (2) Cognitive traits (e.g., emotion, memorability) reside in isolated, property-specific datasets, hindering a unified model for joint multi-dimensional intervention. (3) Achieving robust, zero-shot intervention that generalizes across open-domain content remains elusive.

In this work, we present CogBlender, a unified framework for **continuous and multi-dimensional cognitive property intervention** in text-to-image generation. The framework enables fine-grained modulation of cognitive attributes throughout the generative process while maintaining the generalization of open-domain content. We instantiate CogBlender across four representative and widely-studied cognitive dimensions: (1) *Valence (V)*, capturing the perceived pleasantness of an image; (2) *Arousal (A)*, reflecting the intensity of the elicited emotional response; (3) *Dominance (D)*, indicating the observer's perceived sense of agency (low: being submissive or overwhelmed vs. high: feeling influential or in control); and (4) *Memorability (M)*, a high-order cognitive attribute measuring the likelihood that an image will be retained in human memory. All the four attributes are psychologically meaningful, and exhibit inter-subject consistency across observers [Bylinskii et al. 2021; Kosti et al. 2017; Kurdi et al. 2017]. Additionally, V, A, and D are widely utilized to model emotional states [Bradley and Lang 1994]. We model each cognitive dimension as a continuous, normalized variable within the range $[0, 1]$. This formulation establishes a principled foundation for cognitive-driven image generation and provides a scalable pathway for extending CogBlender to a broader class of cognitive properties.

CogBlender takes a text prompt and a multi-dimensional cognitive score vector as inputs and achieves precise cognitive intervention by reformulating the flow-matching process [Lipman et al. 2023], which generates images by modeling the velocity field that directs the probability flow from noise to clear image, within the state-of-the-art FLUX.2 model [Labs 2025]. Specifically, we formally define the *Cognitive Space*, representing human cognitive properties, and the *Semantic Manifold*, representing the semantics of the images. To bridge these domains, we establish a mapping by identifying a set of *Cognitive Anchors* that serve as the fundamental bases. By rewriting the input prompt to align with these anchors, we delineate the boundaries of the semantic manifold. Then we achieve continuous semantic interpolation with these cognitive anchors as basis points, thus enabling precise and fine-grained intervention over the resulting cognitive effects. Extensive experiments demonstrate that CogBlender achieves superior precision and continuity in cognitive intervention. The main technical contributions of CogBlender are:

- We define the task of *Multi-Dimensional Continuous Cognitive Intervention* in text-to-image generation, shifting the paradigm from static prompting to a dynamic, multi-dimensional control space. To address this, we propose CogBlender, a framework capable of fine-grained cognitive modulation.
- We establish a mapping between the multi-dimension cognitive space and the semantic manifold. We identify a set of cognitive anchors as the fundamental basis points and introduce a polarization mechanism to rewrite input prompt towards multi-dimensional cognitive property polarization, to represent the semantics of cognitive anchor.
- We devise an interpolation strategy that integrates cognitive intervention directly into the flow-matching process. By reformulating the velocity field as a weighted combination of anchor-conditioned trajectories, we achieve smooth interpolation on the semantic manifold while preserving the semantic consistency.

2 Related Works

In this section, we review related research from two aspects: conditional image generation and cognitive properties of images.

2.1 Conditional Image Generation

Conditional image generation aims to synthesize images guided by diverse signals, ranging from text prompts [Labs 2025; Podell et al. 2024], camera poses [He et al. 2025], to reference images [Mou et al. 2024; Ye et al. 2023; Zhang et al. 2023]. Beyond these, some research has explored image generation guided by high-level attributes. In representative domains such as emotional image generation [Dang et al. 2025; Jia et al. 2025; Yang et al. 2024, 2025b], existing works have explored both categorical and continuous control. For instance, EmoGen [Yang et al. 2024] aligns categorical emotion space with semantic space, while EmotiCrafter [Dang et al. 2025] incorporates continuous Valence-Arousal values for nuanced guidance. Further advancing this, EmoFeedback2 [Jia et al. 2025] leverages reinforcement learning to refine emotional fidelity. Regarding image memorability, GANalyze [Goetschalckx et al. 2019] pioneered the use of

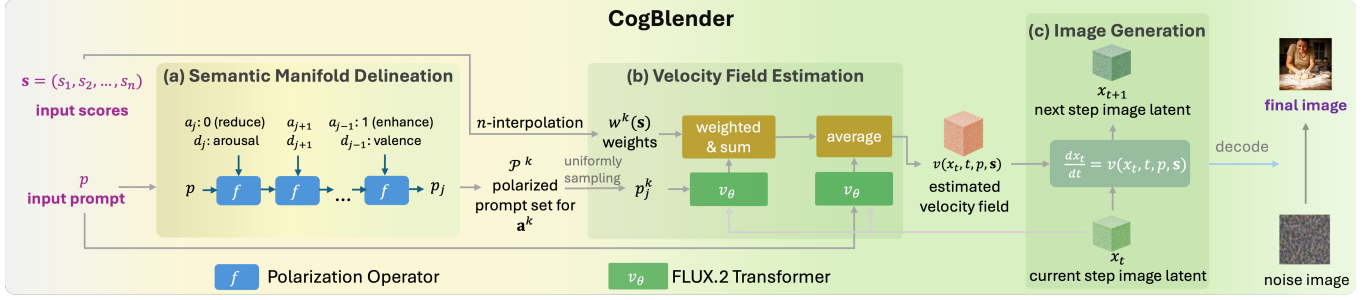


Fig. 2. Overview of CogBlender framework.

cognitive predictors to navigate latent spaces along specific "memorability directions."

Existing research has primarily focused on isolated attributes, leaving the compounded effects of multi-dimensional cognitive properties unexplored. To bridge this gap, our work, CogBlender, proposes a unified framework that enables continuous and multi-dimensional cognitive intervention.

2.2 Cognitive Properties of Images

Cognitive properties of images refer to psychologically evaluated attributes emerging from the interaction between visual stimuli and human cognitive processes, which serve as critical mediators that shape human behaviors [Kim et al. 2021; Szczepanowski et al. 2013].

Emotion is one of the most fundamental cognitive appraisals elicited by images. Psychological research commonly models emotion in the valence–arousal–dominance (V-A-D) space [Bradley and Lang 1994; Kosti et al. 2017; Kurdi et al. 2017], representing pleasantness, intensity, and sense of control, respectively. Another property, memorability, directly determines whether visual information is retained over time and has been demonstrated to be a stable, image-level property [Bylinskii et al. 2021]. Closely related to this is recallability, referring to the ease with which specific visual details and structural information can be accurately reconstructed from memory, primarily explored within the data visualization community [Wang et al. 2022] that has yet to be fully extended to natural imagery and general visual design. Properties such as aesthetics [Murray et al. 2012] and interestingness [Constantin et al. 2021] have also been the subject of systematic study and predictive modeling, indicating algorithmic predictability. However, these dimensions are more susceptible to individual experiences, cultural nuances, and personal aesthetic priors, often leading to higher inconsistency in human perception.

Overall, we select valence-arousal-dominance and memorability as the primary dimensions to validate our framework. Notably, our architecture is designed to be dimension-agnostic, providing a scalable foundation for extending cognitive intervention.

3 CogBlender

In this section, we first introduce the fundamental concepts of the *Cognitive Space* and the *Semantic Manifold*, which together provide the theoretical foundation underlying our approach. We then present the technical details of CogBlender, describing its core components and implementation.

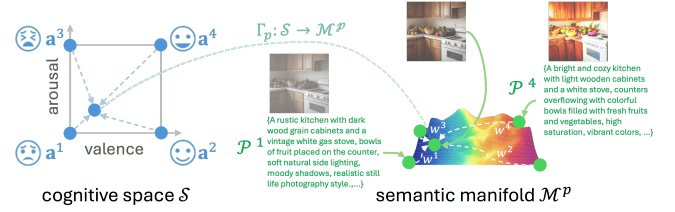


Fig. 3. Visualization of cognitive space \mathcal{S} , semantic manifold \mathcal{M}^P , cognitive anchors $\{a^k\}$ and the polarized prompt sets $\{P^k\}$, utilizing a two-dimensional Valence-Arousal space as an example.

3.1 Cognitive Space and Semantic Manifold

To enable precise and continuous control over cognitive properties in image generation, we must first explicitly model the relationship between cognitive attributes and visual semantics. To this end, we introduce the concept of **Cognitive Space** and **Semantic Manifold** and build their connection via **Cognitive Anchors** in the context of an input prompt p .

Cognitive Space. The cognitive space \mathcal{S} is a continuous, multi-dimensional representation of human psychological responses to visual stimuli (e.g., images). Specifically, \mathcal{S} is modeled as an n -dimensional unit hypercube, $\mathcal{S} = [0, 1]^n$, enabling continuous control over multiple cognitive attributes. Each point $s = (s_1, \dots, s_n) \in \mathcal{S}$ corresponds to a target cognitive profile, where each coordinate s_i represents the normalized intensity of the i -th cognitive property, such as valence, arousal, or memorability.

Semantic Manifold. The semantic manifold \mathcal{M}^P denotes the subspace of textual descriptions that preserve the core semantic identity of a base prompt p while allowing variation in descriptive attributes. Each point $p' \in \mathcal{M}^P$ corresponds to a distinct semantic instance. For example, if p is "a mountain lake", a point $p' \in \mathcal{M}^P$ could be "a vibrant mountain lake under a warm morning sun," which maintains the underlying semantics while introducing additional descriptive nuance. We hypothesize that \mathcal{M}^P exhibits a continuous structure, and further assume the existence of a continuous mapping $\Gamma_p : \mathcal{S} \rightarrow \mathcal{M}^P$, which associates each cognitive score vector with a corresponding semantic realization conditioned on the prompt p . This assumption enables continuous interpolation and modulation of cognitive attributes within the semantic space.

Cognitive Anchors. To delineate the boundaries of the cognitive space \mathcal{S} , we define the vertices of its n -dimensional hypercube as

Cognitive Anchors. These 2^n vertices are encoded as binary vectors $\mathbf{a}^k \in \{0, 1\}^n$, each representing an extreme cognitive state in which every dimension is either minimally or maximally expressed. For example, in a two-dimensional cognitive space spanned by *Valence* and *Arousal*, with the base prompt p given as “a valley”, the cognitive anchor $\mathbf{a}^1 = (0, 0)$ represents a state of low pleasure (i.e., low valence) and low energy (i.e., low arousal). Its semantic could be expressed as prompt “a desolate, misty valley rendered in cold, muted tones.” In contrast, the anchor $\mathbf{a}^4 = (1, 1)$ corresponds to a high-valence, high-arousal state, whose semantics can be represented as “a vibrant, sun-drenched valley filled with blooming flowers”.

3.2 Algorithm Overview

The CogBlender framework (Fig. 2) is designed to generate images that exhibit targeted cognitive effects. The generation is conditioned on two primary inputs: (1) a base text prompt p , and (2) a target cognitive score vector $\mathbf{s} = (s_1, \dots, s_n) \in \mathcal{S}$, where $\mathcal{S} = [0, 1]^n$ denotes the n -dimensional cognitive space and each s_i specifies the desired intensity of the i -th cognitive property. **The core idea is to fine-tune p according to \mathbf{s} to achieve precise control over image generation while maintaining the generalization and fidelity of the underlying pre-trained model.** Directly encoding continuous cognitive interventions within a single prompt, however, is inherently challenging due to (1) the discrete and symbolic nature of natural language, and (2) the absence of datasets suitable for training models capable of jointly rewriting prompts across multiple cognitive dimensions. To address these challenges, we propose a velocity-field-based cognitive intervention algorithm that is seamlessly integrated into the flow-matching framework [Lipman et al. 2023].

The proposed technique consists of three steps: (1) **Semantic Manifold Delineation:** we first delineate a continuous semantic manifold \mathcal{M}^p conditioned on p (Fig. 2(a)) by systematically polarizing (i.e., rewriting towards the cognitive extremes) the input prompt p . This manifold provides a structured and differentiable semantic foundation for performing fine-grained, continuous cognitive intervention during the generation process; (2) **Velocity Field Estimation:** next, we estimate the semantic velocity field for image generation by performing continuous interpolation over \mathcal{M}^p , guided by the input cognitive score vector \mathbf{s} (Fig. 2(b)). This interpolation induces a smooth and differentiable mapping from the cognitive score space to latent semantic representations, which serves as the conditioning signal for downstream flow-based image synthesis; (3) **Image Generation:** finally, the image I is synthesized within the flow-matching framework by integrating the estimated velocity field v (Fig. 2(c)). This integration steers the denoising trajectory toward image latents that are jointly consistent with the original input prompt p and the target cognitive score vector \mathbf{s} .

3.3 Semantic Manifold Delineation

We explore an effective method for precisely delineating the extreme boundaries of the semantic manifold \mathcal{M}^p conditioned on the input prompt p based on a given cognitive space $\mathcal{S} = [0, 1]^n$. The core idea is to polarize (i.e., rewrite) the input prompt p based on each of the cognitive anchors $\mathbf{a}^k \in \{0, 1\}^n$ to produce a set of prompts

that semantically represents the boundary of the underlying semantic manifold \mathcal{M}^p . Here, each cognitive anchor $\mathbf{a}^k = (a_1, a_2, \dots, a_n)$ is defined as an n -dimensional binary vector, where $a_i \in \{0, 1\}$ specifies the pole of the i -th cognitive dimension, with 0 and 1 respectively indicating the negative and positive extremes of the corresponding cognitive attribute. For instance, in a two-dimensional Valence–Arousal cognitive space, this construction yields a set of anchor prompts that explicitly instantiate the four extreme semantic configurations formed by the Cartesian product of {maximal, minimal} valence and {maximal, minimal} arousal.

We implement the above idea by sequentially polarizing (i.e., rewriting) the input prompt p along each cognitive dimension using a polarization operator f . The operator f is implemented via instruction fine-tuning of a large language model (Qwen3-14B [Yang et al. 2025a]) and is designed to rewrite a prompt with respect to a specified cognitive dimension d . Formally, f is defined as

$$p' = f_d^a(p) \quad (1)$$

where $a \in \{0, 1\}$ denotes the pole of the cognitive dimension d toward which the prompt p is polarized, corresponding to the enhancement ($a = 1$) or attenuation ($a = 0$) of d .

In the sequential prompt rewriting process, each step is conditioned on a specific cognitive dimension, which can cause the final prompt to be disproportionately biased toward the last intervened dimension. To mitigate this effect, we introduce a counterbalanced rewriting mechanism, in which the order of dimension-wise rewritings for each cognitive anchor \mathbf{a}^k is systematically rotated according to a Latin square over the set of cognitive dimensions. Consequently, for each anchor, a set of n prompts is generated (denoted as \mathcal{P}^k), collectively capturing the extreme semantic variations of the input prompt p with respect to the cognitive attributes defined by the corresponding cognitive anchor. In other words, the prompt set \mathcal{P}^k serves as the semantic representation of the k -th cognitive anchor, instantiated in the contextual semantics of the input prompt p .

Specifically, for each cognitive anchor \mathbf{a}^k , we generate a set of polarized prompts \mathcal{P}^k by following different rewriting orders:

$$\mathcal{P}^k = \{p_1^k, p_2^k, \dots, p_n^k\}, \quad k \in \{1, \dots, 2^n\}, \quad (2)$$

where p_j^k denotes a prompt produced via sequential, dimension-wise rewriting, with the rewriting process initialized from the j -th cognitive dimension. The order is rotated based on a Latin square to enumerate all possible combination orders, which can be formally described as:

$$p_j^k = \left(f_{d_{j-1}}^{a_{j-1}^k} \circ f_{d_{j-2}}^{a_{j-2}^k} \circ \dots \circ f_{d_1}^{a_1^k} \circ f_{d_n}^{a_n^k} \circ \dots \circ f_{d_j}^{a_j^k} \right) (p), \quad (3)$$

where f_d^a is the polarization operator, \circ represents functional composition.

3.4 Velocity Field Estimation

To achieve a precise cognitive intervention, we interpolate across the extreme boundary of the semantic manifold \mathcal{M}^p (delineated by $\{\mathcal{P}^k\}$) to effectively map the input cognitive score vector \mathbf{s} to a target intermediate semantic state in \mathcal{M}^p . To implement this idea, rather than directly interpolating in the text embedding space produced by LLM, which is usually non-linear and semantically

unstable, we perform continuous cognitive control in the velocity-field domain of flow matching. Velocity fields have been proven to provide a smoother and more well-structured space for semantic interpolation, enabling stable and precise cognitive intervention during image generation [Ho and Salimans 2021; Labs 2025].

Specifically, a velocity field $v(x_t, t, p, \mathbf{s})$ is estimated, where x_t denotes the noisy image latent at continuous time t in the flow-matching process; t is the time variable governing the generative trajectory; p represents the input text prompt; and \mathbf{s} denotes the target cognitive score vector. Formally, it can be calculated as:

$$v(x_t, t, p, \mathbf{s}) = \frac{1}{2} \left(\sum_{k=1}^{2^n} w_k(\mathbf{s}) \cdot \hat{v}(x_t, t, \mathcal{P}^k) + v_\theta(x_t, t, p) \right) \quad (4)$$

where v_θ is the pretrained FLUX.2 transformer to predict the velocity field; the term $v_\theta(x_t, t, p)$ represents the velocity predicted from the original base prompt p , which serves as a structural constraint to preserve the fundamental semantic identity of the image. To ensure computational efficiency during the inference stage, we adopt the ‘‘stochastic approximation’’ strategy to estimate $\hat{v}(x_t, t, \mathcal{P}^k)$. Specifically, at each timestep t , we approximate the velocity by uniformly sampling a single prompt p_j^k from \mathcal{P}^k :

$$\hat{v}(x_t, t, \mathcal{P}^k) \approx v_\theta(x_t, t, p_j^k), \quad p_j^k \sim \text{Uniform}(\mathcal{P}^k) \quad (5)$$

In equation (4), $w_k(\mathbf{s})$ denotes the interpolation weight, representing the contribution of the k -th cognitive anchor \mathbf{a}^k based on its proximity to \mathbf{s} . It can be formally computed as follows:

$$w_k(\mathbf{s}) = \prod_{i=1}^n \left(s_i a_i^k + (1 - a_i^k)(1 - s_i) \right) \quad (6)$$

where a_i^k denotes the polarization action of the i -th value in cognitive anchor \mathbf{a}^k , and $\mathbf{s} = (s_1, \dots, s_n) \in [0, 1]^n$ represents the target cognitive score vector.

3.5 Image Generation

Based on the interpolated velocity field $v(x_t, t, p, \mathbf{s})$, we generate an image I by solving the following probability flow Ordinary Differential Equation (ODE) introduced in the flow-matching framework:

$$\frac{dx_t}{dt} = v(x_t, t, p, \mathbf{s}), \quad t \in [0, 1], \quad x_0 \sim \mathcal{N}(\mathbf{0}, \mathbf{1}) \quad (7)$$

The solution is obtained by integrating the velocity field from initial Gaussian noise x_0 to the final image latent x_1 , which is then mapped to the pixel space via a pretrained VAE decoder:

$$I = \text{Decoder} \left(x_0 + \int_0^1 v(x_t, t, p, \mathbf{s}) dt \right) \quad (8)$$

For further details, please refer to the supplementary material, which includes extended dataset construction procedures, operator training configurations, and parameters used for image generation.

4 Experiments and Results

We evaluate the proposed method through two primary tasks: (1) continuous emotional image content generation (C-EICG) and (2) memorability-aware image generation. In addition, we conducted comprehensive ablation studies to quantify the contribution of each

Table 1. Quantitative comparison on C-EICG. We report the mean \pm standard deviation for each metric. **Bold** indicates the best performance. \uparrow denotes higher is better, and \downarrow denotes lower is better.

	Method	CLIPScore \uparrow	CLIPQA \uparrow	V-Err \downarrow	A-Err \downarrow	D-Err \downarrow
V-A	EmotiCrafter	17.544 \pm 3.219	0.861 \pm 0.076	0.235 \pm 0.154	0.301 \pm 0.185	–
	FLUX.2	26.928 \pm 2.561	0.867 \pm 0.096	0.304 \pm 0.175	0.308 \pm 0.181	–
	CogBlender	26.434 \pm 2.417	0.912 \pm 0.069	0.277 \pm 0.168	0.295 \pm 0.175	–
V-A-D	FLUX.2	26.939 \pm 2.519	0.873 \pm 0.094	0.342 \pm 0.196	0.347 \pm 0.219	0.359 \pm 0.215
	CogBlender	26.346 \pm 2.378	0.909 \pm 0.069	0.324 \pm 0.191	0.341 \pm 0.211	0.357 \pm 0.215

component in our framework. Finally, we present extensive qualitative results to demonstrate the robustness and broad applicability of our approach across diverse generation scenarios.

4.1 Experiment I: C-EICG

We first validate the CogBlender’s capability to intervene in the emotional properties of generated images. Our evaluation considers two widely adopted affective representations: the two-dimensional Valence–Arousal (V–A) space and the three-dimensional Valence–Arousal–Dominance (V–A–D) space.

Testsets and Baselines. To ensure prompt diversity, we construct a test set of 100 prompts synthesized using GPT-4o, covering both human-centric and non-human-centric scenes. We compare our method against two baselines (additional details regarding the baselines are provided in the supplementary material): (1) **EmotiCrafter**, the state-of-the-art C-EICG model [Dang et al. 2025] specifically developed for generating emotional images via a prompt and a pair of continuous V–A scores; (2) **FLUX.2** [Labs 2025]: a prompt-engineering baseline that explicitly encodes V–A–D scores into textual prompts and then applies the FLUX.2 text-to-image model.

Metrics. To quantitatively assess the performance of CogBlender, we adopt three categories of evaluation metrics:

- **Text–Image Alignment (CLIPScore):** We evaluate the semantic consistency between the generated images and the input prompts [Hessel et al. 2021]. It is a cosine similarity between image and text embeddings. Higher scores indicate stronger text–image alignment.
- **Emotion Fidelity (V/A/D-Err):** We quantify the accuracy of emotional intervention using the mean absolute error (MAE) between the target emotional scores and those predicted from the generated images. Lower V/A/D-Err values indicate more precise emotional control. To obtain the predicted scores, we fine-tune a Qwen3-VL model with a regression head to map images to continuous Valence, Arousal, and Dominance (V/A/D) values. The resulting predictor demonstrates high reliability, achieving Pearson correlation coefficients of 0.91, 0.87, and 0.88 for V, A, and D, respectively, when evaluated against human-annotated ground truth.
- **Visual Quality (CLIPQA):** We evaluate the visual quality of generated images using CLIPQA [Wang et al. 2023], a reference-free image quality assessment metric, where higher scores indicate better perceptual quality¹.

¹Although distribution-based metrics such as Fréchet Inception Distance(FID) [Heusel et al. 2017] are widely adopted, they are less suitable in our setting as our objective is controlled image generation rather than matching a target image distribution.

Quantitative and Qualitative Analysis. We present a comprehensive comparison in Tab. 1 and Fig. 5.

Emotion Intervention. As summarized in Tab. 1, CogBlender achieves consistently strong and often superior emotional fidelity across both V-A and V-A-D settings. Although EmotiCrafter attains a marginally lower error in the valence dimension, CogBlender delivers the best overall performance across all cognitive axes, reflecting more balanced and reliable emotional control. As shown in Fig. 5, our method enables precise and stable modulation of valence, arousal, and dominance. Notably, EmotiCrafter’s slight advantage in valence control comes at the cost of reduced semantic alignment and limited effectiveness in arousal modulation, while FLUX.2 fails to achieve meaningful control over either arousal or dominance.

Visual Quality and Fidelity. As reported in Tab. 1, all evaluated methods preserve high visual quality, with CogBlender achieving the best overall performance. Compared with FLUX.2, the superior visual fidelity of CogBlender can be attributed to its explicit modeling of emotional attributes, which encourages richer visual details and more expressive scene compositions—an effect consistent with prior findings on emotion-driven image synthesis [Zhu et al. 2024].

Qualitative comparisons in Fig. 5 further substantiate these observations. While both CogBlender and FLUX.2 generate clear, high-resolution images, EmotiCrafter exhibits a noticeably constrained and stylized visual appearance, limiting photorealistic diversity. Moreover, as illustrated in Fig. 5(a), CogBlender effectively modulates fine-grained visual cues (e.g., lighting intensity and contrast), demonstrating its ability to achieve cognitively guided yet visually faithful image generation.

Text-Image Alignment. As summarized in Tab. 1, CLIPScore evaluation shows that although FLUX.2 achieves the highest score due to its large-scale pretraining, CogBlender incurs only a marginal and practically negligible performance drop, while preserving strong semantic fidelity to the input prompt. In contrast, EmotiCrafter exhibits substantially lower CLIPScores, indicating weaker text-image alignment. These trends are consistent with the qualitative results in Fig. 5. For instance, for the prompt “*wooden cabin*”, EmotiCrafter frequently fails to preserve the primary subject, producing images in which the cabin is missing or visually ambiguous. This comparison underscores the ability of CogBlender to maintain semantic consistency while enabling continuous cognitive intervention.

User Study. We verify the effectiveness of the emotional intervention of CogBlender through a controlled user study. Specifically, we evaluate whether human ratings align with the target intensities along Valence (V), Arousal (A), and Dominance (D).

Stimuli. We constructed three stimulus sets, one per dimension. For each set, we generated 15 images spanning five target intensity levels, with three distinct exemplars per level ($5 \times 3 = 15$). In total, the study included 45 images (15 per dimension).

Procedure and Task. We recruited 20 college students (12 female; aged 22-28) as participants. Participants first completed a brief tutorial introducing the definitions of V/A/D and the 5-point Likert rating scheme, with examples illustrating each scale value for each dimension. Participants then completed the main task in three blocks, one per dimension. In each block, they viewed the 15 images

Table 2. User study result of emotional intervention. Lower MAE and higher Pearson’s r indicate better alignment. All correlations are statistically significant ($p < 0.001$).

Dimension	MAE	Pearson’s r
Valence	0.145± 0.045	0.851 ***
Arousal	0.178± 0.058	0.784 ***
Dominance	0.166± 0.075	0.767 ***

corresponding to that dimension and rated only the target dimension on a 5-point Likert scale. Within each block, image order was independently randomized for each participant.

Analysis & Results. We normalized the 5-point Likert ratings to the $[0, 1]$ interval to match the target intensity levels. For each dimension, we quantified the alignment between target intensities and participant ratings using two metrics: (1) mean absolute error (MAE) and (2) Pearson’s correlation coefficient r .

As shown in Table 2, the results indicate strong agreement between generated images and target emotional interventions across all three dimensions. All correlations are statistically significant $p < 0.001$, with MAE values consistently below 0.18 on the normalized scale. These findings demonstrate that CogBlender can reliably produce images that convey intended emotional content along valence, arousal, and dominance dimensions.

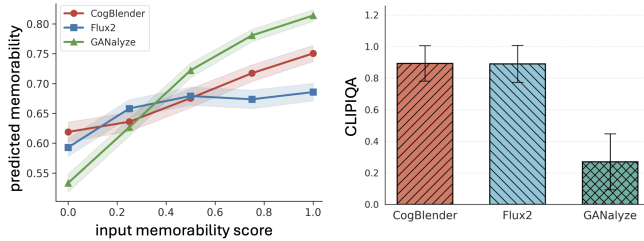
4.2 Experiment II: Memorability-Aware Image Generation

This experiment examines CogBlender’s ability to modulate users’ memorability responses to generated images.

Baselines. We compare CogBlender against two representative baselines: (1) **GANalyze** [Goetschalckx et al. 2019], a pioneering approach that manipulates cognitive properties by traversing the latent space of a pre-trained GAN (e.g., BigGAN). GANalyze controls a learned transformation direction using a scalar parameter $\alpha \in [-0.2, 0.2]$, where larger values of α correspond to increased image memorability. For fair comparison, we linearly rescale α to the range $[0, 1]$ to match the conditioning domain used by all evaluated methods. (2) **FLUX.2** [Labs 2025], a prompt-based baseline that relies on explicit prompt engineering to steer image generation. We construct its prompts following the same protocol as in Experiment I.

Quantitative Analysis. For GANalyze, we randomly select 20 object categories and generate 5 images per category, following its original evaluation protocol. For all other methods, we reuse the text prompts from Experiment I to generate the test images. Image memorability is predicted using MemNet [Khosla et al. 2015]. Quantitative results are summarized in Fig. 4.

As shown in the target-predicted memorability curves (Fig. 4(a)), GANalyze exhibits a steeper response slope. However, FLUX.2 demonstrates unstable behavior, including negatively correlated intervals where increased target memorability does not lead to higher predicted scores. In contrast, CogBlender achieves a strong and approximately linear alignment between target and predicted memorability scores, indicating reliable and continuous cognitive intervention. Notably, all methods struggle to synthesize images with extremely low memorability, reflecting the intrinsic difficulty of suppressing salient visual cues.



(a) predicted vs. input memorability scores (b) comparison of image quality
Fig. 4. Quantitative evaluation of memorability intervention.

In terms of visual quality (Fig. 4(b)), both CogBlender and FLUX.2 maintain high image fidelity, whereas GANalyze suffers from substantial quality degradation (CLIPQA score < 0.3).

Qualitative Analysis. Fig. 6 shows that CogBlender achieves superior semantic fidelity and more effective memorability modulation than the baselines. GANalyze increases memorability mainly through low-level visual manipulations (e.g., scaling or contrast), which often introduce semantic drift and structural artifacts, as shown in the *building* and *dog* examples in Fig 6. In contrast, CogBlender preserves scene semantics while adjusting higher-level cues such as lighting, composition, and object saliency.

FLUX.2 exhibits limited perceptual variation across memorability levels (e.g., *market square* in Fig 6), whereas CogBlender produces clear and continuous visual transitions. For example, in the *stop sign* case in Fig 6, memorability is progressively enhanced via stronger color contrast and improved text clarity. In more complex scenes (e.g., *child drawing* in Fig 6), CogBlender guides attention by modulating global contrast and focal sharpness, aligning with known mechanisms of human memory encoding.

4.3 Ablation Study

We conduct an ablation study to evaluate the impact of each core component in CogBlender. Fig. 8 provides qualitative comparisons on the C-EICG task over the V-A grid, together with the corresponding inference time.

The Effectiveness of Polarization Operator. We remove the polarization operator and instead use a pretrained Qwen3 prompt rewriter without training. As shown in Fig. 8(a), the generated images remain largely unchanged across the V-A grid, indicating weak sensitivity to the target cognitive score. This suggests that the polarization operator f is critical for translating numerical V-A scores into corresponding changes in the semantic content of the generated images, enabling reliable emotional control.

The Effectiveness of Cognitive Anchors. We evaluate the contribution of cognitive anchors by removing the vertex anchors in the V-A space. Instead of relying on these anchors, we polarize each dimension independently and directly compose their effects during interpolation within the velocity field. As shown in Fig. 8(b), this variant produces severe over-exposure and saturation. These results suggest that cognitive anchors define the boundary of the cognitive space. Without them, low-level visual changes (e.g., brightness and color intensity) are easily amplified, leading to over-exposure or saturation and reduced reliability.

The Effectiveness of the Base-Prompt Velocity $v_\theta(x_t, t, p)$.

We ablate the base-prompt velocity by removing $v_\theta(x_t, t, p)$ predicted from the original base prompt p . As shown in Fig. 8(c), although this variant strengthens the emotional intervention, it introduces semantic distortion and pronounced lighting fluctuations, especially at extreme cognitive scores. These results indicate that the base-prompt velocity serves as a structural constraint that preserves visual stability and semantic fidelity during inference.

The Effectiveness of the Random Sampling Strategy.

We ablate the random sampling strategy by averaging the velocity fields over all polarized anchor prompts. As shown in Fig. 8(d), this variant retains strong emotional intervention capability but incurs a substantial increase in inference time (40.36s per image). In contrast, random sampling in CogBlender maintains comparable controllability while reducing latency to 22.60s per image, nearly halving the inference time and improving practical efficiency.

4.4 Generality to Diverse Styles.

We further examine the generality of CogBlender under diverse artistic styles and scene compositions. As shown in Fig. 9(a), CogBlender remains effective across these styles, which produces coherent images that preserve the target style while responding consistently to the specified cognitive interventions. For instance, the traditional Chinese painting example maintains its brushwork and composition as the cognitive score increases.

4.5 Applications

CogBlender supports practical use cases enabled by its continuous cognitive intervention mechanism. First, CogBlender can facilitate **advertising and promotional content creation** by jointly modulating emotion and memorability to match desired communication goals. As shown in Fig. 9(b) and Fig. 1, emotion and memorability can be controlled simultaneously without sacrificing semantic consistency. Second, CogBlender is useful for **video synthesis and storyboarding**, where fine-grained navigation in the cognitive space is needed to produce smooth transitions. Fig. 10 demonstrates stable interpolation between disparate cognitive states along a specified trajectory. Finally, CogBlender naturally extends from generation to **image editing**. As shown in Fig. 7, given a reference image, our method selectively adjusts cognitive properties while preserving the reference structure and semantic identity. For details, please refer to the Supplementary Material.

4.6 Discussion

While CogBlender achieves promising results on this challenging task, several limitations remain. First, the training-free design improves generality but increases inference-time computation; future work could distill our framework into a more efficient forward process. Second, controllability is limited when the input semantics inherently carry strong cognitive signals (e.g., injuries, accidents, or striking animals), pushing them toward the opposite attribute often requires semantic edits that break the original content. Finally, prompt-level polarization cannot precisely specify every visual detail, so fine-grained appearance factors may be difficult to control;

adding latent-space constraints may improve fidelity but could require training and reduce zero-shot generality.

5 Conclusion

In this work, we introduce CogBlender, a unified framework for generating images with target cognitive effects. The key idea of CogBlender is to construct a semantic manifold conditioned on the input prompt via a polarization operator, and to estimate a cognitively conditioned velocity field by interpolating over this manifold, enabling stable intervention while preserving the semantic identity specified by the prompt. Extensive experiments show that CogBlender reliably aligns generated images with both user prompts and target cognitive scores, generalizes across diverse styles and scenes. We believe this work bridges cognitive intervention with image synthesis, paving the way for more interpretable generation. We will release our code and data to foster further research.

References

- Margaret M Bradley and Peter J Lang. 1994. Measuring emotion: the self-assessment manikin and the semantic differential. *Journal of behavior therapy and experimental psychiatry* 25, 1 (1994), 49–59.
- Zoya Bylinskii, Lore Goetschalckx, Anelise Newman, and Aude Oliva. 2021. Memorability: An image-computable measure of information utility. In *Human perception of visual information: Psychological and computational perspectives*. 207–239.
- Patrick Cavanagh. 2011. Visual cognition. *Vision research* 51, 13 (2011), 1538–1551.
- Yiming Chen, Junlin Han, Tianyi Bai, Shengbang Tong, Filippos Kokkinos, and Philip Torr. 2025. From Pixels to Feelings: Aligning MLLMs with Human Cognitive Perception of Images. arXiv:2511.22805
- Mihai Gabriel Constantin, Liviu-Daniel Ștefan, Bogdan Ionescu, Ngoc QK Duong, Claire-Hélène Demarty, and Mats Sjöberg. 2021. Visual interestingness prediction: A benchmark framework and literature review. *International Journal of Computer Vision* 129, 5 (2021), 1526–1550.
- Shengqi Dang, Yi He, Long Ling, Ziqing Qian, Nanxuan Zhao, and Nan Cao. 2025. Emoticafter: Text-to-emotional-image generation based on valence-arousal model. In *Proceedings of the IEEE/CVF International Conference on Computer Vision*. 15218–15228.
- Trent M Davis and Wilma A Bainbridge. 2023. Memory for artwork is predictable. *Proceedings of the National Academy of Sciences* 120, 28 (2023), e2302389120.
- Charles D Gilbert and Wu Li. 2013. Top-down influences on visual processing. *Nature reviews neuroscience* 14, 5 (2013), 350–363.
- Lore Goetschalckx, Alex Andonian, Aude Oliva, and Phillip Isola. 2019. GANalyze: Toward visual definitions of cognitive image properties. In *Proceedings of the IEEE/CVF International Conference on Computer Vision*. 5744–5753.
- Hao He, Yinghao Xu, Yuwei Guo, Gordon Wetzstein, Bo Dai, Hongsheng Li, and Ceyuan Yang. 2025. CameraCtrl: Enabling Camera Control for Video Diffusion Models. In *Proceedings of International Conference on Learning Representations*.
- Jack Hessel, Ari Holtzman, Maxwell Forbes, Ronan Le Bras, and Yejin Choi. 2021. Clipscore: A reference-free evaluation metric for image captioning. In *Proceedings of Conference on Empirical Methods in Natural Language Processing*. 7514–7528.
- Martin Heusel, Hubert Ramsauer, Thomas Unterthiner, Bernhard Nessler, and Sepp Hochreiter. 2017. Gans trained by a two time-scale update rule converge to a local nash equilibrium. *Advances in neural information processing systems* 30 (2017).
- Jonathan Ho and Tim Salimans. 2021. Classifier-Free Diffusion Guidance. In *NeurIPS 2021 Workshop on Deep Generative Models and Downstream Applications*.
- Jingyang Jia, Kai Shu, Gang Yang, Long Xing, Xun Chen, and Aiping Liu. 2025. EmoFeedback²: Reinforcement of Continuous Emotional Image Generation via LVM-based Reward and Textual Feedback. arXiv:2511.19982
- Aditya Khosla, Akhil S Raju, Antonio Torralba, and Aude Oliva. 2015. Understanding and predicting image memorability at a large scale. In *Proceedings of the IEEE international conference on computer vision*. 2390–2398.
- Minjeong Kim, Jung-Hwan Kim, Minjung Park, and Jungmin Yoo. 2021. The roles of sensory perceptions and mental imagery in consumer decision-making. *Journal of Retailing and Consumer Services* 61 (2021), 102517.
- Ronak Kosti, Jose M. Alvarez, Adria Recasens, and Agata Lapedriza. 2017. EMOTIC: Emotions in Context Dataset. In *Proceedings of the IEEE Conference on Computer Vision and Pattern Recognition (CVPR) Workshops*. 61–69.
- Benedek Kurdi, Shayn Lozano, and Mahzarin R Banaji. 2017. Introducing the open affective standardized image set (OASIS). *Behavior research methods* 49, 2 (2017), 457–470.
- Black Forest Labs. 2025. FLUX.2: Frontier Visual Intelligence. <https://bfl.ai/blog/flux-2>.
- Yaron Lipman, Ricky T. Q. Chen, Heli Ben-Hamu, Maximilian Nickel, and Matthew Le. 2023. Flow Matching for Generative Modeling. In *Proceedings of International Conference on Learning Representations*.
- Chong Mou, Xintao Wang, Liangbin Xie, Yanze Wu, Jian Zhang, Zhongang Qi, and Ying Shan. 2024. T2i-adapter: Learning adapters to dig out more controllable ability for text-to-image diffusion models. In *Proceedings of the AAAI Conference on Artificial Intelligence*, Vol. 38. 4296–4304.
- Naila Murray, Luca Marchesotti, and Florent Perronnin. 2012. AVA: A large-scale database for aesthetic visual analysis. In *Proceedings of IEEE Conference on Computer Vision and Pattern Recognition*. 2408–2415.
- Ulric Neisser. 2014. *Cognitive psychology: Classic edition*. Psychology press.
- Dustin Podell, Zion English, Kyle Lacey, Andreas Blattmann, Tim Dockhorn, Jonas Müller, Joe Penna, and Robin Rombach. 2024. SDXL: Improving Latent Diffusion Models for High-Resolution Image Synthesis. In *Proceedings of International Conference on Learning Representations*.
- Felix Septianto, Sheng Ye, and Gavin Northey. 2021. The effectiveness of advertising images in promoting experiential offerings: An emotional response approach. *Journal of Business Research* 122 (2021), 344–352.
- Remigiusz Szczepanowski, Jakub Traczyk, Michał Wierzbchoń, and Axel Cleeremans. 2013. The perception of visual emotion: comparing different measures of awareness. *Consciousness and cognition* 22, 1 (2013), 212–220.
- Jianyi Wang, Kelvin CK Chan, and Chen Change Loy. 2023. Exploring clip for assessing the look and feel of images. In *Proceedings of the AAAI Conference on Artificial Intelligence*, Vol. 37. 2555–2563.
- Yao Wang, Chuhan Jiao, Mihai Băce, and Andreas Bulling. 2022. VisRecall: Quantifying information visualisation recallability via question answering. *IEEE Transactions on Visualization and Computer Graphics* 28, 12 (2022), 4995–5005.
- An Yang, Anfeng Li, Baosong Yang, Beichen Zhang, Binyuan Hui, Bo Zheng, Bowen Yu, Chang Gao, Chengen Huang, Chenxu Lv, et al. 2025a. Qwen3 Technical Report. arXiv:2505.09388
- Jingyuan Yang, Jiawei Feng, and Hui Huang. 2024. EmoGen: Emotional Image Content Generation with Text-to-Image Diffusion Models. In *Proceedings of the IEEE/CVF Conference on Computer Vision and Pattern Recognition*. IEEE, 6358–6368.
- Jingyuan Yang, Weibin Luo, and Hui Huang. 2025b. EmoCtrl: Controllable Emotional Image Content Generation. arXiv:2512.22437
- Hu Ye, Jun Zhang, Sibio Liu, Xiao Han, and Wei Yang. 2023. IP-Adapter: Text Compatible Image Prompt Adapter for Text-to-Image Diffusion Models. arXiv:2308.06721
- Lvmin Zhang, Anyi Rao, and Maneesh Agrawala. 2023. Adding Conditional Control to Text-to-Image Diffusion Models. In *Proceedings of the IEEE/CVF International Conference on Computer Vision*. 3813–3824.
- Tong Zhu, Leida Li, Pengfei Chen, Jinjian Wu, Yuzhe Yang, and Yaqian Li. 2024. Emotion-aware hierarchical interaction network for multimodal image aesthetics assessment. *Pattern Recognition* 154 (2024), 110584.

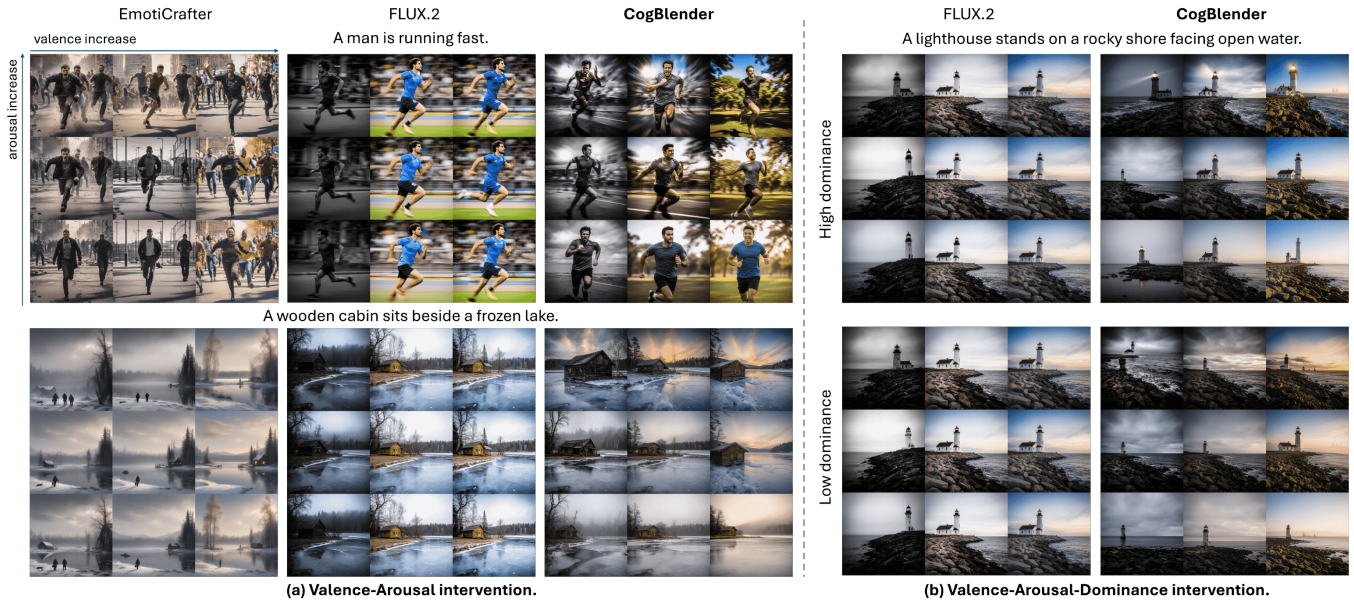


Fig. 5. Qualitative comparison of emotion-conditioned image generation.



Fig. 6. Qualitative comparison of memorability-aware image generation.



Fig. 7. Reference-based image editing for cognitive intervention.

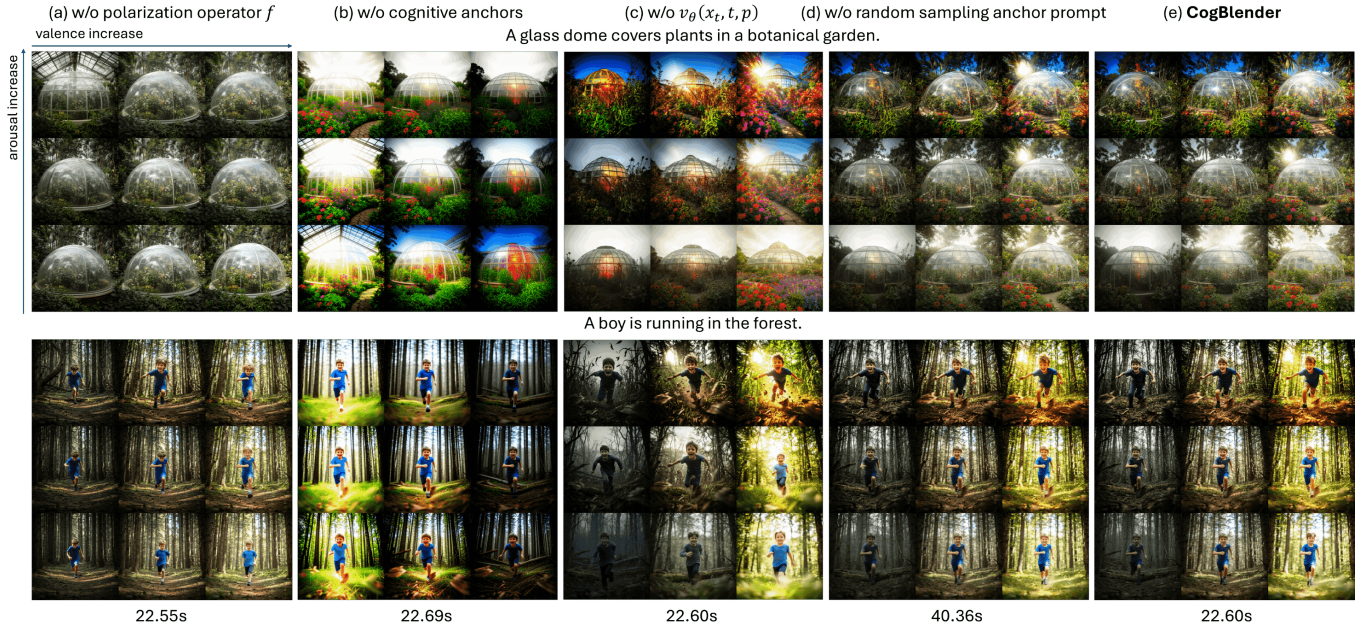


Fig. 8. Ablation study on the Valence-Arousal conditional image generation task. We evaluate the contribution of each component. The average time for per image generation is reported below each corresponding method.



Fig. 9. Extended results across diverse domains. (a) Generalization to various artistic styles (e.g., oil painting) and different scenes. (b) Dual-attribute control, demonstrating simultaneous and decoupled modulation of emotional dimensions (V/A) and memorability.



Fig. 10. Continuous cognitive interpolation. Smooth transition from high valence and arousal (V=0.7, A=0.7) to low valence and arousal (V=0.1, A=0.1). The results showcase a consistent shift in visual atmosphere and emotional impact along a continuous trajectory while maintaining subject stability.